

1 **TITLE: Corner height influences center of mass**  
2 **kinematics and path trajectory during turning**

3 **KEYWORDS:** gait, turning, speed, biomechanics, center of mass, COM, turning  
4 angle,

5 **AUTHORS:** Peter C. Fino, Department of Mechanical Engineering, Virginia  
6 Polytechnic Institute and State University

7 Thurmon E. Lockhart, Grado Department of Industrial and  
8 Systems Engineering, Virginia Polytechnic Institute and State  
9 University

10 **CORRESPONDING AUTHOR:** Thurmon E. Lockhart, Grado Department of  
11 Industrial and Systems Engineering, Virginia Polytechnic Institute and State  
12 University, 557 Whittemore Hall, MC 0118, Blacksburg, VA 24061, (540)-231-  
13 9088, lockhart@vt.edu

14 **WORD COUNT:** 4184

15 **Abstract**

16 Despite the prevalence of directional changes during every-day gait, relatively little is known  
17 about turning compared to straight gait. While the whole body center-of-mass (COM) movement  
18 during straight gait is well characterized, the COM trajectory, and the factors that influence it,  
19 are less established for turning. This study investigated the influence of a corner's height on the  
20 COM trajectory as participants walked around the corner. Ten participants ( $25.3 \pm 3.74$  years)  
21 performed both  $90^\circ$  step and spin turns to the left at self-selected slow, normal, and fast speeds  
22 while walking inside a marked path. A pylon was placed on the inside corner of the path. Four  
23 different pylon heights were used to correspond to heights of everyday objects: 0 cm (no object),  
24 63 cm (box, crate), 104 cm (desk, table, counter), 167 cm (shelf, cabinet). Obstacle height was  
25 found to significantly affect the COM trajectory. Taller obstacles resulted in more distance  
26 between the corner and the COM, and between the corner and the COP. Taller obstacles also  
27 were associated with greater curvature in the COM trajectory, indicating a smaller turning radius  
28 despite the constant  $90^\circ$  corner. Taller obstacles correlated to an increased required coefficient of  
29 friction (RCOF) due to the smaller turning radii. Taller obstacles also tended towards greater  
30 mediolateral (ML) COM-COP angles, contrary to the initial hypothesis. Additionally, the COM  
31 was found to remain outside the base of support (BOS) for the entire first half of stance phase for  
32 all conditions indicating a high risk of falls resulting from slips.

### 33 **Introduction**

34 Human gait has been a widely researched area especially concerning slips, trips, and falls.  
35 However, the majority of research has examined straight gait even though daily activities  
36 necessitate directional changes. Turning and non-straight steps make up approximately 35-45%  
37 of all steps (Glaister et al., 2007a) yet has received relatively little attention compared to straight  
38 gait. An individual's whole body center-of-mass (COM) trajectory has been well characterized  
39 during straight gait (Gard et al., 2004; Granata and Lockhart, 2008; Lee and Farley, 1998; Lee  
40 and Chou, 2006; Lockhart et al., 2003; MacKinnon and Winter, 1993; Orendurff et al., 2004) but  
41 is less understood during turning.

42 Turning is distinctly different than straight walking (Glaister et al., 2008; Hicheur and Berthoz,  
43 2005). Turning requires a much larger required coefficient of friction (RCOF) to prevent slips  
44 (Fino and Lockhart, 2014) and has a higher incidence of falls resulting from slips (Yamaguchi et  
45 al., 2012a) than straight walking due to the lateral displacement of the COM relative to the base  
46 of support (BOS). The radius of the turn affects the orientation of the head and trunk while  
47 walking (Sreenivasa et al., 2008). The COM is also affected by the turning radius with larger  
48 turning angles resulting in greater COM displacement (Hollands et al., 2001) as well as  
49 decreased walking velocity (Dias et al., 2013). Increasing the walking speed has a similar  
50 relationship, increasing the COM displacement outside the BOS (Orendurff et al., 2006).

51 To date, no study has examined how the geometry of an object affects the COM around a turn.  
52 During turning, individuals tend to "lean in" to the turn to compensate for the centripetal force  
53 necessary to make a turn (Courtine and Schieppati, 2003). While the degree to which individuals  
54 lean depends on speed (Orendurff et al., 2006) and turning radius (Hollands et al., 2001), the

55 response if this “lean in” angle is obstructed by an obstacle is unknown. Previous studies have  
56 used objects to demark a corner (Grasso et al., 1998) or prevent participants from crossing  
57 through a corner (Glaister et al., 2008; Glaister et al., 2007b), but there is currently no knowledge  
58 concerning how the object’s shape or size influences the participants’ kinematics. Our earlier  
59 analysis reported no effect of obstacle height on RCOF during the push-off phase of gait (Fino  
60 and Lockhart, 2014) but did not examine other phases of the turn nor reported COM trajectories.  
61 Given that most turns in a crowded environment are to avoid obstacles (Glaister et al., 2007a), it  
62 is worth investigating whether the geometry of those obstacles impacts the resulting maneuver  
63 and influences fall risk. This knowledge, while important for researchers wishing to examine  
64 turning gait, may also prove useful in the design of pedestrian environments by providing  
65 guidelines for the height or size of barricades, posts, tables, and walls in order to maximize  
66 pedestrian flow and reduce the chance of slips and falls.

67 This study observed the impact of an object’s height on the COM trajectory at slow, normal, and  
68 fast walking speeds while making a 90° turn. Our primary hypothesis was that taller obstacles  
69 would restrict the amount of “lean-in,” where “lean in” was defined as the mediolateral (ML)  
70 component of the COM-COP angle,  $\theta_{ML}$ . Additionally, we hypothesized that taller obstacles  
71 would result in wider turns with larger path curvature and greater clearance between the obstacle  
72 and the COM or COP (i.e. foot placement). The RCOF was also examined during the weight  
73 acceptance phase of the turn with a hypothesis that increased obstacle height would result in  
74 increased RCOF. Additionally,  $\theta_{ML}$ , the COM and COP clearance, and the RCOF were  
75 hypothesized to increase with faster speeds (Fino and Lockhart, 2014; Orendurff et al., 2006),  
76 with the COM and COP clearance and  $\theta_{ML}$  expected to be greater for step turns than for spin  
77 turns (Taylor et al., 2005).

## 78 **Methods**

### 79 Participants

80 Ten healthy adults (7 male, 3 female) 18-45 years of age (mean  $\pm$  std dev = 25.3  $\pm$  3.74 years),  
81 were recruited from Virginia Tech and the surrounding community for the study. Participants  
82 were informed of the protocol and signed an informed consent form prior to the experiment.  
83 Participants were excluded if they had any history of balance disorders, dizziness,  
84 musculoskeletal injury the past year affecting normal gait, any neurological disorders, one or  
85 more concussions within the past year, and / or significant visual impairment. The complete  
86 protocol was approved by the Institutional Review Board at Virginia Tech.

### 87 Experimental Procedure

88 The full procedure was reported by Fino and Lockhart (2014). Briefly, participants walked along  
89 a 0.75 m wide marked path with a 90° turn. The path was straight for 3.5 m followed by a 90°  
90 left turn into a 2.5 m long straight segment. The beginning and end of the corner path were  
91 marked with start and stop lines, respectively. A 10 cm diameter pylon was placed on the inside  
92 of the 90° corner as the obstacle. Four different pylon heights were used corresponding to  
93 heights of everyday objects: 0 cm (no object), 63 cm (box, crate), 104 cm (desk, table, counter),  
94 and 167 cm (shelf, cabinet). The floor surface was covered in a Micropore tape (3M, St. Paul,  
95 MN 55144-1000, USA) to prevent slipping while turning the corner, especially at fast speeds.  
96 Prior testing revealed gait adjustments and slips when performing the task. The tape successfully  
97 increased the available friction of the floor allowing the participants' natural actions to be  
98 observed without any adaptations (Fino and Lockhart, 2014). Participants wore their own athletic  
99 shoes throughout the experiment. An overhead view of the set-up is shown in Figure 1.

Figure 1.

100  
101 Three-dimensional kinematics were measured using a six-camera Pro-Reflex motion analysis  
102 system (Qualisys Track Manager version 1.6.0.163, Qualisys AB, Gothenburg, Sweden) and 35  
103 infrared-reflective markers placed bilaterally over the first, second, and fifth metatarsal heads,  
104 medial and lateral malleolus, calcaneus, medial and lateral femoral condyle, anterior superior  
105 iliac spine, trochanter, iliac crest, clavicle, acromioclavicular (AC) joint, lateral humeral condyle,  
106 ulnar styloid, third metacarpal head, ear, and top of head. A marker was also placed on top of the  
107 corner pylon directly over the inside corner of the path. Two force plates (AMTI #  
108 BP6001200100, AMTI Force and Motion, Watertown, MA 02472, USA) (Bertec #K80102,  
109 Type 45550-08, Bertec Corporation, OH 43212, USA) were embedded into the walkway just  
110 before and after the corner pylon. All data was sampled at 100 Hz.

111 Participants were instructed to walk normally inside the path until they reached the stop line and  
112 to avoid hitting the pylon. The participants were instructed to walk at one of three speeds: normal  
113 (NW), slower than their normal pace (SW), and “as fast as possible without running or jogging”  
114 (FW). Warm-up trials were used to adjust the subjects starting position such that their turning  
115 limb landed on the corner force plate. The participants performed three straight gait trials,  
116 followed by 24 turning trials for each speed. The turning trials were divided into four blocks, one  
117 for each obstacle height. For each obstacle height, participants performed three step turns and  
118 three spin turns, where a step turn was defined as a turn away from the stance limb and a spin  
119 turn is defined as a turn toward the same side of the stance limb (Taylor et al., 2005). To  
120 eliminate order effects, speed, obstacle height, and step turn versus spin turn order was rotated  
121 for each participant (Fino and Lockhart, 2014). A total of 72 turning trials and nine straight

122 walking trials were recorded for each participant: three spin turns and three step turns for each of  
123 the four obstacle heights at each of the three speeds and three straight trials for each speed.

#### 124 Data Analysis

125 Data from all ten participants were analyzed. Trials in which the participant stepped multiple  
126 times on the force plate or only partially stepped on the force plate were excluded from the  
127 analysis. A total of 291 of the 720 trials were excluded for this reason (148 slow trials, 84  
128 normal, and 59 fast). These excluded trials occurred across all ten participants. The 3-  
129 dimensional marker data and the force plate data were filtered using a 5 Hz 2<sup>nd</sup> order low-pass  
130 Butterworth filter. Due to a systematic obstruction of the motion capture cameras' view of the  
131 markers during the second half of the stance phase, kinematic data from only the first half of  
132 each stance phase was analyzed. All analysis was performed using MATLAB (MATLAB and  
133 Statistics Toolbox Release 2013b, The MathWorks, Inc., Natick, Massachusetts, USA).

#### 134 *COM Clearance and COP Distance*

135 The COM was calculated using individual body segment mass and COM location from the  
136 reflective markers at the segment endpoints (De Leva, 1996). The COM clearance was calculated  
137 as the distance in the horizontal plane from the COM to the corner pylon as shown in Figure 2.  
138 Due to the different pylon heights, a vertical projection of the corner pylon was used. This  
139 projection extended upward to the COM height. The ground reactive forces (GRF) were recorded  
140 by the force plate and used to calculate the COP according to the force plate manufacturer  
141 (Bertec Corporation, OH 43212, USA). The COP distance was calculated as the distance from  
142 the COP at weight acceptance to the corner pylon.

143 Figure 2.

144 *Required Coefficient of Friction*

145 The frictional demand RCOF was also calculated as

146 
$$RCOF = \frac{F_{horizontal}}{F_{vertical}} \quad (1)$$

147 where  $F_{vertical}$  is the vertical force  $F_z$  and  $F_{horizontal}$  is the resultant sum of  $F_x$  and  $F_y$ ,

148 
$$F_{horizontal} = \sqrt{F_x^2 + F_y^2} . \quad (2)$$

149 Maximum RCOF values were extracted from the first half of the stance phase where the stance  
150 limb contacted the force plate. The maximum RCOF during the first half of the stance phase  
151 corresponded to the RCOF at weight acceptance. Immediately following heel contact and  
152 preceding toe-off, large RCOF values have previously been reported but do not result in slips  
153 (Redfern et al., 2001). The large RCOF values are products of extremely small vertical GRFs,  
154 which inflate the RCOF values. In practice, however, the opposite limb supports the majority of  
155 the body weight. Thus, slipping the foot supporting little body weight does not result in the  
156 macroscopic slips associated with slip and fall accidents. To prevent these high RCOF values  
157 which do not typically result in slips and falls from distorting the RCOF necessary to prevent a  
158 slip, only RCOF values where the vertical force was greater than 50 N were compared (Fino and  
159 Lockhart, 2014; Yamaguchi et al., 2012b). Stance time was defined as the time from heel contact  
160 to the push-off / toe-off phase of the gait cycle (i.e. the vertical force dropped below 50 N as the  
161 toe pushed off the ground) during the directional change.

162 *COM-COP Angle*



163 The amount of “lean in” was defined as the ML COM-COP angle,  $\theta_{ML}$ . It was calculated as a  
164 component of the total COM-COP angle,  $\theta$ , between the vertical axis and the line connecting the  
165 COM to the COP, (Yamaguchi et al., 2012b)

$$166 \quad \Theta = \tan^{-1} \frac{\sqrt{(x_{COP}-x_{COM})^2+(y_{COP}-y_{COM})^2}}{z_{COM}} \quad (3)$$

167 where  $x_{COP}$ ,  $y_{COP}$  are the x and y coordinates of the COP and  $x_{COM}$ ,  $y_{COM}$ , and  $z_{COM}$  are the x,  
168 y, and z coordinates of the COM. The ML COM-COP angle,  $\theta_{ML}$ , shown in Figure 3 was  
169 calculated as the ML component of  $\theta$  using the orientation of the pelvis to construct a body fixed  
170 reference frame (Glaister et al., 2007b). The body fixed reference frame was constructed using  
171 the vector from the mean of the iliac crest and trochanter markers on the right side to the left  
172 side.  $\theta_{ML}$  was calculated at the same time as the RCOF at weight acceptance.

173 Figure 3.

#### 174 *COM Curvature*

175 Whereas the turning angle was specified at  $90^\circ$ , the turning radius of the COM may change  
176 based on  $\theta_{ML}$  and the amount of the outlined path the participants’ actually utilize. The curvature  
177 of the COM trajectory is a more accurate indicator of the true turning radius. To calculate the  
178 curvature of the COM trajectory, a least-squares quadratic polynomial equation was fitted to the  
179 COM trajectory in the horizontal plane using MATLAB. Taking the second derivative of this  
180 function with respect to the x axis

$$181 \quad \frac{d^2 f(x)}{dx^2} = \kappa = \frac{1}{r} \quad (5)$$

182 yielded a constant curvature  $\kappa$  equal to the inverse of the radius,  $\frac{1}{r}$ . The magnitude of the  
183 curvature  $\kappa$  was calculated for each COM trajectory.

#### 184 *Approach Speed and Turning Speed*

185 The turning speed was defined as the resultant instantaneous COM velocity at weight  
186 acceptance. It was calculated at the same instant as the RCOF at weight acceptance. The  
187 approach speed was defined as the speed of the participant as he approached the corner prior to  
188 any deceleration. It was calculated from the resultant instantaneous COM velocity at weight  
189 acceptance one stride before the turn.

#### 190 Statistical Analysis

191 Univariate descriptive statistics of the COM clearance, COP distance, RCOF, and  $\theta_{ML}$  were  
192 calculated at each speed, height, and turning strategy. To determine the relationship between  
193 COM clearance, COP radius, RCOF,  $\theta_{ML}$ , and curvature to speed, height, and turning  
194 strategy, we fit generalized estimating equation (GEE) models that account for the within subject  
195 correlation among each subject's trials. We selected the compound symmetry covariance  
196 structure as the most appropriate structure for our data after comparing several models using the  
197 Akaike information criterion. Model assumptions were validated using the distributions of the  
198 residuals for each model. Curvature had a skewed distribution and was thus log transformed in  
199 order to satisfy the models' assumptions. Contrasts between each obstacle height were performed  
200 for each outcome. Trial, two-way and three-way interaction effects were also examined using  
201 type 3 tests for fixed effects with significant interactions retained in the final model. A 0.05  
202 significance level was used throughout this analysis. All analysis was performed in SAS 9.4  
203 (SAS Institute Inc., Cary, NC, USA).

## 204 **Results**

### 205 Descriptive Results

206 Univariate descriptive statistics are summarized in Table 1. The average height and weight of the  
207 participants was  $1.78 \pm 0.11$  meters tall (mean  $\pm$  std dev) and  $79.97 \pm 12.39$  kg, respectively.

208 Mean approach speeds and turning speeds are summarized in Table 2. Weight acceptance was at  
209 an average of 10% of stance phase. Values for  $\theta_{ML}$  are plotted in Figure 4 for the first half of  
210 stance phase.

211 Table 1.

212 Table 2.

213 Figure 4.

214 The average trajectories of the COM and the left and right foot COMs are shown in Figures 4-6  
215 for each obstacle height, speed, and strategy. The COM remained outside the BOS during the  
216 first half of stance for every condition. The average COM trajectories for each variable are  
217 overlaid in Figure 8 for a direct curvature comparison. All quadratic fits had a  $R^2$  value greater  
218 than 0.9.

219 Figure 5.

220 Figure 6.

221 Figure 7.

222 Figure 8.

223 GEE Model Results

224 From the results of the GEE model presented in Table 3, higher obstacle heights resulted in  
225 statistically significant increases in COM clearance, COP distance, RCOF, and curvature.  
226 Statistically significant differences in  $\theta_{ML}$  existed between the lowest (0 cm) and tallest (167 cm)  
227 obstacle heights. Though not statistically significant, a difference in  $\theta_{ML}$  between the 0 cm and  
228 104 cm heights was also found. Contrasts revealed no additional statistical differences in  $\theta_{ML}$   
229 between any pairwise comparisons of height, though slight differences between the 104 cm and  
230 167 cm heights ( $p=0.0633$ ) and between 63 cm and 167 cm heights ( $p=0.1079$ ) were noted.  
231 Significant differences were found between all height-wise contrasts for COM clearance,  
232 curvature, and COP distance ( $p<0.0001$ ). Contrasts also showed significantly different RCOF  
233 values between heights 104 cm and 167 cm ( $p=0.0123$ ) with all other contrasts not statistically  
234 significant.

235 COM clearance, RCOF, curvature, and  $\theta_{ML}$  at self-selected slow and fast speeds were  
236 significantly different compared to normal speeds. Turning strategy significantly affected all  
237 outcomes.

238 There was a significant interaction between speed and turning strategy for curvature ( $p=0.0072$ ).  
239 Spin turns had decreased curvature compared to step turns at slow speeds but increased curvature  
240 with respect to step turns at fast speeds. No other significant two or three-way interactions  
241 between speed, obstacle height, and turning strategy ( $p>0.05$ ) and no significant trial effects were  
242 found. Measured approach and turning speeds for slow, normal, and fast speeds were  
243 significantly different from one another ( $p<0.0001$ ). No differences were found in turning speeds  
244 across obstacle height ( $p=0.79$ ) or turning strategy ( $p=0.27$ ).

245  
246  
247  
248  
249  
250  
251  
252  
253  
254  
255  
256  
257  
258  
259  
260  
261  
262  
263  
264  
265  
266

Table 3.

**Discussion**

This study investigated the impact of a corner obstacle’s height on the kinematics during a turn. We found increased obstacle heights caused participants to give more distance between themselves and the corner. In essence, taller obstacles resulted in wider, sharper turns. Fast speeds, regardless of obstacle height, resulted in less COM clearance and narrower turns compared to normal or slow walking speeds. Similarly, spin turns brought the COM closer to the corner than step turns.

Most prior studies investigating turning used walking paths or destination cues with no obstacle (Akram et al., 2010; Chang and Kram, 2007; Courtine and Schieppati, 2003; Hicheur and Berthoz, 2005; Hicheur et al., 2007; Hicheur et al., 2005; Jindrich et al., 2006; Olivier et al., 2008; Orendurff et al., 2006; Patla et al., 1999; Patla et al., 1991; Pham et al., 2007; Taylor et al., 2005; Yamaguchi et al., 2012a, b), while other obstacle circumvention studies used 2 m high pylons (Gérin-Lajoie et al., 2008; Gérin-Lajoie et al., 2006; Gérin-Lajoie et al., 2007; Vallis and McFadyen, 2003, 2005), 1.53 m tall poles (Glaister et al., 2008; Glaister et al., 2007b) or pedestrian barricades (Dias et al., 2013). The present results indicate the height of the corner could be an important factor in the study design. Hicheur et al. (2007) showed that when given a target direction, individuals’ planar trajectories tend to follow a stereotyped behavior that minimizes jerk and snap (Pham et al., 2007). Fajen and Warren (2003) also provided a dynamical model of steering and route selection based on a two-dimensional, top-down, environment. Fajen and Warren (2003) acknowledged the inability of the system to model obstacles of varying lengths and widths. Our results suggest the height of the obstacle is also an important

267 characteristic, necessitating a three-dimensional model to accurately describe obstacle avoidance.  
268 Similarly, the “personal space” characterized by Gérin-Lajoie et al. (2008) would be more  
269 accurately defined as a three-dimensional vector space rather than in two-dimensions.

270 Examining the trajectories of the whole body COM compared to the left and right foot COMs,  
271 we found that on average the whole body COM remains outside the BOS for the entire first half  
272 of stance phase *regardless of speed, turning strategy, or obstacle height*. This is in stark contrast  
273 to previous results which showed the COM only exited the BOS on spin turns (Taylor et al.,  
274 2005) or at fast speeds (Orendurff et al., 2006). It is important to note that Taylor et al. (2005)  
275 instructed participants to perform quick/abrupt turn in the minimum amount of time, consistent  
276 with the theory that turning is an avoidance strategy as characterized by Patla et al. (1991). In  
277 reality, most turns in everyday locomotion occur over several steps (Fajen and Warren, 2003;  
278 Glaister et al., 2007a). In accordance, the subjects in our study were not instructed to make  
279 abrupt turns, but instead to turn the corner naturally.

280 This new result has large implications for slips and falls. Because the COM remains outside the  
281 BOS for the entire first half of stance phase, slips during this weight acceptance phase are more  
282 likely to result in falls (Yamaguchi et al., 2012a). Furthermore, the RCOF values found during  
283 this weight acceptance phase of turning exceeded the RCOF values for normal walking of  $\mu \cong$   
284 0.20 (Cham and Redfern, 2002; Redfern et al., 2001). This suggests that not only are slips more  
285 likely to occur while turning compared to normal walking (Fino and Lockhart, 2014; Yamaguchi  
286 et al., 2012b), but slips during the weight acceptance phase of turning may be more likely to  
287 result in falls than straight walking slips because of the COM displacement outside the BOS. In  
288 addition, we found the RCOF at weight acceptance differed between obstacle heights, suggesting  
289 the surrounding objects, not simply the available coefficient of friction from the shoe-floor

290 interface, may influence the risk of slipping. While a previous analysis showed no differences  
291 between obstacle heights at the time of push-off (Fino and Lockhart, 2014) this difference  
292 between obstacle heights is most likely due to the different path curvatures caused by the  
293 obstacle.

294 When walking around a corner, the centripetal force,  $F_c$ , is provided by the frictional force  
295 characterized by the individual's body weight  $W$  and the RCOF  $\mu$ . The centripetal force required  
296 to change direction is proportional to the velocity squared,  $v^2$ , and the inverse of the radius,  $r$ ,  
297 also known as the curvature,  $\kappa$

$$298 \quad F_c = \mu W = \frac{mv^2}{r} = mv^2\kappa . \quad (6)$$

299 Therefore, the RCOF is proportional to the velocity squared and the magnitude of the curvature

$$300 \quad \mu \propto v^2\kappa . \quad (7)$$

301 When compared with the curvature results, the differences in RCOF by obstacle height become  
302 clear. As obstacle height increased, it forced the COM further from the corner and increased the  
303 curvature. This increased curvature is most likely a cause of the increased RCOF. However, the  
304 increased RCOF at weight acceptance for faster speeds, despite a lower curvature, is caused by  
305 the proportionality to  $v^2$ , which overcame the decrease in  $\kappa$ . The increased  $\theta_{ML}$  also contributed  
306 to the increased RCOF values observed during taller obstacle trials (Yamaguchi et al., 2012b).

307 These results suggest that the radius of the turn, not the angle of the turn as presented by  
308 Yamaguchi et al. (2012a), is the critical factor in slip and fall risk during turning. However, if all  
309 are performed over the same distance, larger turning angles will necessarily result in a smaller  
310 turning radius. Thus the turning angle will reflect the actual turning radius.

311 The curvature and RCOF results have implications for designing pedestrian environments. In  
312 designing pedestrian walkways and areas, it may be important to consider not only the turning  
313 angle of paths (Dias et al., 2013) and the floor space of obstacles but also the height of  
314 barricades, railings, tables, posts, and walls that will impact the pedestrian path. Posts prohibiting  
315 vehicular traffic on pedestrian areas should be constructed high enough to be visible and  
316 effective, but as low as possible to reduce the effect on pedestrians. Besides reducing congestion,  
317 such design considerations may also be able to reduce the likelihood of slips and falls by  
318 maintaining low curvature paths to reduce the RCOF.

319 Interestingly, across the obstacle heights and turning strategies, an increased COM clearance  
320 paired with an increased COP distance. However, this was not true for speed. As speed  
321 increased, the COP radius increased, but the COM clearance decreased. This would indicate  
322 greater  $\theta_{ML}$  angles at faster speeds consistent with results from Orendurff et al. (2006). Indeed,  
323 this result was observed; faster speeds utilized a greater  $\theta_{ML}$ . While we predicted the obstacle  
324 height would alter the COM by *limiting*  $\theta_{ML}$ , our results tended towards the opposite. An increase  
325 in obstacle height resulted in *larger*  $\theta_{ML}$  values. Notably, only the lowest and highest heights  
326 were statistically different in terms of  $\theta_{ML}$ . However, this difference is peculiar as we expected  
327 taller obstacles would inhibit the lateral motion of the participants and restrict the degree to  
328 which the participants could lean over the obstacle and into the turn. This larger  $\theta_{ML}$  for the taller  
329 obstacle heights may have been caused by an anticipation of the smaller turning radius described  
330 above. Participants may have increased  $\theta_{ML}$  for taller obstacles because of the increased  
331 centripetal force of smaller radii. By leaning into the turn, they would have reduce the net  
332 overturning moment by balancing the moment due to friction with the moment due to their COM  
333 displacement. For this study,  $\theta_{ML}$  was only calculated at weight acceptance, therefore this result



334 may only be true during the weight acceptance phase of the turn. From Figure 4, it appears that  
335 examining the maximum  $\theta_{ML}$  may yield different results than when extracting the  $\theta_{ML}$  from  
336 weight acceptance (~10% stance). Furthermore, the motor control strategy was not investigated  
337 in this study. Future research should explore this entire result in greater detail.

338 Overall, these results show obstacle height has a distinct effect on navigational strategies. Future  
339 work should investigate whether these effects result in different biomechanical responses such as  
340 increased lateral flexion or trunk roll, as well as the increase of  $\theta_{ML}$  for taller obstacles.

341 This study has two potential limitations. First, the sample size was limited to only 10 people,  
342 although the repeated measures increased the total trial sample size to 429 trials. Second, the  
343 availability of the kinematic marker data from the second half of stance phase was inconsistent.  
344 Due to laboratory space requirements, the motion capture cameras were confined to specified  
345 locations. This presented difficulties in capturing each kinematic marker once the participants  
346 changed directions. Laboratory structures, including the pylon used in the trials, obstructed the  
347 views of the cameras causing some but not all kinematic markers to be lost for periods of time  
348 following the change in direction. Rather than using long spline fits to interpolate these lost data  
349 points, we elected to report only the data which was accurately and consistently captured for  
350 each participant. For this reason, we presented only the first half of stance for all trajectories.  
351 Future analysis should consider the entire stance phase.

### 352 **Conflict of Interest**

353 The authors affirm there are no conflicts of interest.

### 354 **Acknowledgements**

355 This research was supported by the NSF-Information and Intelligent Systems (IIS) and Smart  
356 Health and Wellbeing -1065442 and 1065262. NIOSH (grant #CDC/NIOSHR01-OH009222).

357

358 We would like to thank Nora Fino for help with the statistical analysis. We also want to thank  
359 Rahul Soangra and Chris Frames for the advice throughout the data collection and analysis.

360 Additional thanks goes to Sam Worley and Neal Moriconi for their help during data collection  
361 and processing.

## 362 **References**

- 363 Akram, S.B., Frank, J.S., Chenouri, S., 2010. Turning behavior in healthy older adults: Is there a  
364 preference for step versus spin turns? *Gait Posture* 31, 23-26.
- 365 Cham, R., Redfern, M.S., 2002. Changes in gait when anticipating slippery floors. *Gait Posture* 15, 159-  
366 171.
- 367 Chang, Y.-H., Kram, R., 2007. Limitations to maximum running speed on flat curves. *Journal of*  
368 *Experimental Biology* 210, 971-982.
- 369 Courtine, G., Schieppati, M., 2003. Human walking along a curved path. I. Body trajectory, segment  
370 orientation and the effect of vision. *European Journal of Neuroscience* 18, 177-190.
- 371 De Leva, P., 1996. Adjustments to Zatsiorsky-Seluyanov's segment inertia parameters. *Journal of*  
372 *Biomechanics* 29, 1223-1230.
- 373 Dias, C., Sarvi, M., Shiwakoti, N., Ejtemai, O., Year Experimental Study on Pedestrian Walking  
374 Characteristics through Angled Corridors. In *Australasian Transport Research Forum (ATRF)*, 36th, 2013,  
375 Brisbane, Queensland, Australia.
- 376 Fajen, B.R., Warren, W.H., 2003. Behavioral dynamics of steering, obstacle avoidance, and route  
377 selection. *Journal of Experimental Psychology-Human Perception and Performance* 29, 343-361.
- 378 Fino, P., Lockhart, T., 2014. Required coefficient of friction during turning at self-selected slow, normal,  
379 and fast walking speeds. *Journal of Biomechanics* 47, 1395-1400.
- 380 Gard, S.A., Miff, S.C., Kuo, A.D., 2004. Comparison of kinematic and kinetic methods for computing the  
381 vertical motion of the body center of mass during walking. *Human Movement Science* 22, 597-610.
- 382 Gérin-Lajoie, M., Richards, C.L., Fung, J., McFadyen, B.J., 2008. Characteristics of personal space during  
383 obstacle circumvention in physical and virtual environments. *Gait Posture* 27, 239-247.
- 384 Gérin-Lajoie, M., Richards, C.L., McFadyen, B.J., 2006. The circumvention of obstacles during walking in  
385 different environmental contexts: a comparison between older and younger adults. *Gait Posture* 24,  
386 364-369.
- 387 Gérin-Lajoie, M., Ronsky, J.L., Loitz-Ramage, B., Robu, I., Richards, C.L., McFadyen, B.J., 2007.  
388 Navigational strategies during fast walking: A comparison between trained athletes and non-athletes.  
389 *Gait Posture* 26, 539-545.
- 390 Glaister, B.C., Bernatz, G.C., Klute, G.K., Orendurff, M.S., 2007a. Video task analysis of turning during  
391 activities of daily living. *Gait Posture* 25, 289-294.
- 392 Glaister, B.C., Orendurff, M.S., Schoen, J.A., Bernatz, G.C., Klute, G.K., 2008. Ground reaction forces and  
393 impulses during a transient turning maneuver. *Journal of Biomechanics* 41, 3090-3093.

394 Glaister, B.C., Orendurff, M.S., Schoen, J.A., Klute, G.K., 2007b. Rotating horizontal ground reaction  
395 forces to the body path of progression. *Journal of Biomechanics* 40, 3527-3532.

396 Granata, K.P., Lockhart, T.E., 2008. Dynamic stability differences in fall-prone and healthy adults. *Journal*  
397 *of Electromyography and Kinesiology* 18, 172-178.

398 Grasso, R., Prévost, P., Ivanenko, Y.P., Berthoz, A., 1998. Eye-head coordination for the steering of  
399 locomotion in humans: an anticipatory synergy. *Neuroscience Letters* 253, 115-118.

400 Hicheur, H., Berthoz, A., Year How do humans turn? Head and body movements for the steering of  
401 locomotion Halim Hicheur and Alain Berthoz. In *Humanoid Robots, 2005 5th IEEE-RAS International*  
402 *Conference on*.

403 Hicheur, H., Pham, Q.C., Arechavaleta, G., Laumond, J.P., Berthoz, A., 2007. The formation of trajectories  
404 during goal-oriented locomotion in humans. I. A stereotyped behaviour. *European Journal of*  
405 *Neuroscience* 26, 2376-2390.

406 Hicheur, H., Vieilledent, S., Richardson, M., Flash, T., Berthoz, A., 2005. Velocity and curvature in human  
407 locomotion along complex curved paths: a comparison with hand movements. *Experimental Brain*  
408 *Research* 162, 145-154.

409 Hollands, M., Sorensen, K., Patla, A., 2001. Effects of head immobilization on the coordination and  
410 control of head and body reorientation and translation during steering. *Experimental Brain Research*  
411 140, 223-233.

412 Jindrlich, D.L., Besier, T.F., Lloyd, D.G., 2006. A hypothesis for the function of braking forces during  
413 running turns. *Journal of Biomechanics* 39, 1611-1620.

414 Lee, C.R., Farley, C.T., 1998. Determinants of the center of mass trajectory in human walking and  
415 running. *Journal of Experimental Biology* 201, 2935-2944.

416 Lee, H.-J., Chou, L.-S., 2006. Detection of gait instability using the center of mass and center of pressure  
417 inclination angles. *Archives of Physical Medicine and Rehabilitation* 87, 569-575.

418 Lockhart, T.E., Woldstad, J.C., Smith, J.L., 2003. Effects of age-related gait changes on the biomechanics  
419 of slips and falls. *Ergonomics* 46, 1136-1160.

420 MacKinnon, C.D., Winter, D.A., 1993. Control of whole body balance in the frontal plane during human  
421 walking. *Journal of Biomechanics* 26, 633-644.

422 Olivier, A.-H., Fusco, N., Cretual, A., 2008. Local kinematics of human walking along a turn. *Computer*  
423 *Methods in Biomechanics and Biomedical Engineering* 11, 177-178.

424 Orendurff, M.S., Segal, A.D., Berge, J.S., Flick, K.C., Spanier, D., Klute, G.K., 2006. The kinematics and  
425 kinetics of turning: limb asymmetries associated with walking a circular path. *Gait Posture* 23, 106-111.

426 Orendurff, M.S., Segal, A.D., Klute, G.K., Berge, J.S., Rohr, E.S., Kadel, N.J., 2004. The effect of walking  
427 speed on center of mass displacement. *J Rehabil Res Dev* 41, 829-834.

428 Patla, A.E., Adkin, A., Ballard, T., 1999. Online steering: coordination and control of body center of mass,  
429 head and body reorientation. *Experimental Brain Research* 129, 629-634.

430 Patla, A.E., Prentice, S.D., Robinson, C., Neufeld, J., 1991. Visual control of locomotion: strategies for  
431 changing direction and for going over obstacles. *Journal of experimental psychology. Human perception*  
432 *and performance* 17, 603-634.

433 Pham, Q.C., Hicheur, H., Arechavaleta, G., Laumond, J.P., Berthoz, A., 2007. The formation of trajectories  
434 during goal-oriented locomotion in humans. II. A maximum smoothness model. *European Journal of*  
435 *Neuroscience* 26, 2391-2403.

436 Redfern, M.S., Cham, R., Gielo-Periczak, K., Grönqvist, R., Hirvonen, M., Lanshammar, H., Marpet, M., Pai  
437 IV, C.Y.-C., Powers, C., 2001. Biomechanics of slips. *Ergonomics* 44, 1138-1166.

438 Sreenivasa, M.N., Frissen, I., Souman, J.L., Ernst, M.O., 2008. Walking along curved paths of different  
439 angles: the relationship between head and trunk turning. *Experimental Brain Research* 191, 313-320.

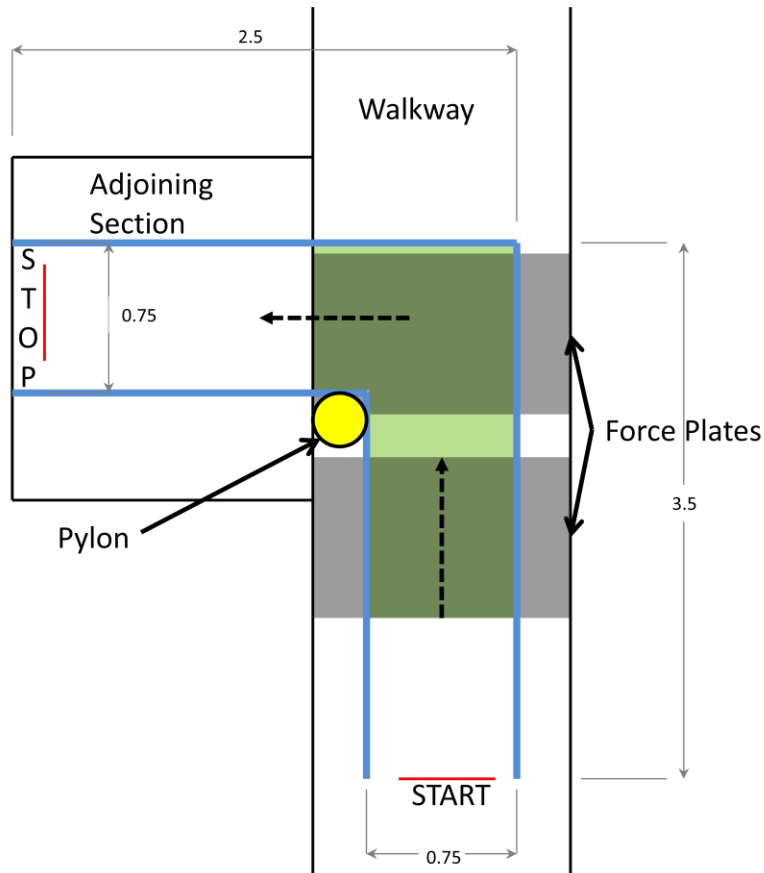
440 Taylor, M., Dabnicki, P., Strike, S., 2005. A three-dimensional biomechanical comparison between  
441 turning strategies during the stance phase of walking. *Human Movement Science* 24, 558-573.

442 Vallis, L.A., McFadyen, B.J., 2003. Locomotor adjustments for circumvention of an obstacle in the travel  
443 path. *Experimental Brain Research* 152, 409-414.  
444 Vallis, L.A., McFadyen, B.J., 2005. Children use different anticipatory control strategies than adults to  
445 circumvent an obstacle in the travel path. *Experimental Brain Research* 167, 119-127.  
446 Yamaguchi, T., Yano, M., Onodera, H., Hokkirigawa, K., 2012a. Effect of turning angle on falls caused by  
447 induced slips during turning. *Journal of Biomechanics* 45, 2624-2629.  
448 Yamaguchi, T., Yano, M., Onodera, H., Hokkirigawa, K., 2012b. Kinematics of center of mass and center  
449 of pressure predict friction requirement at shoe–floor interface during walking. *Gait Posture* 38, 209-  
450 214.

451

452 Figure 1

453

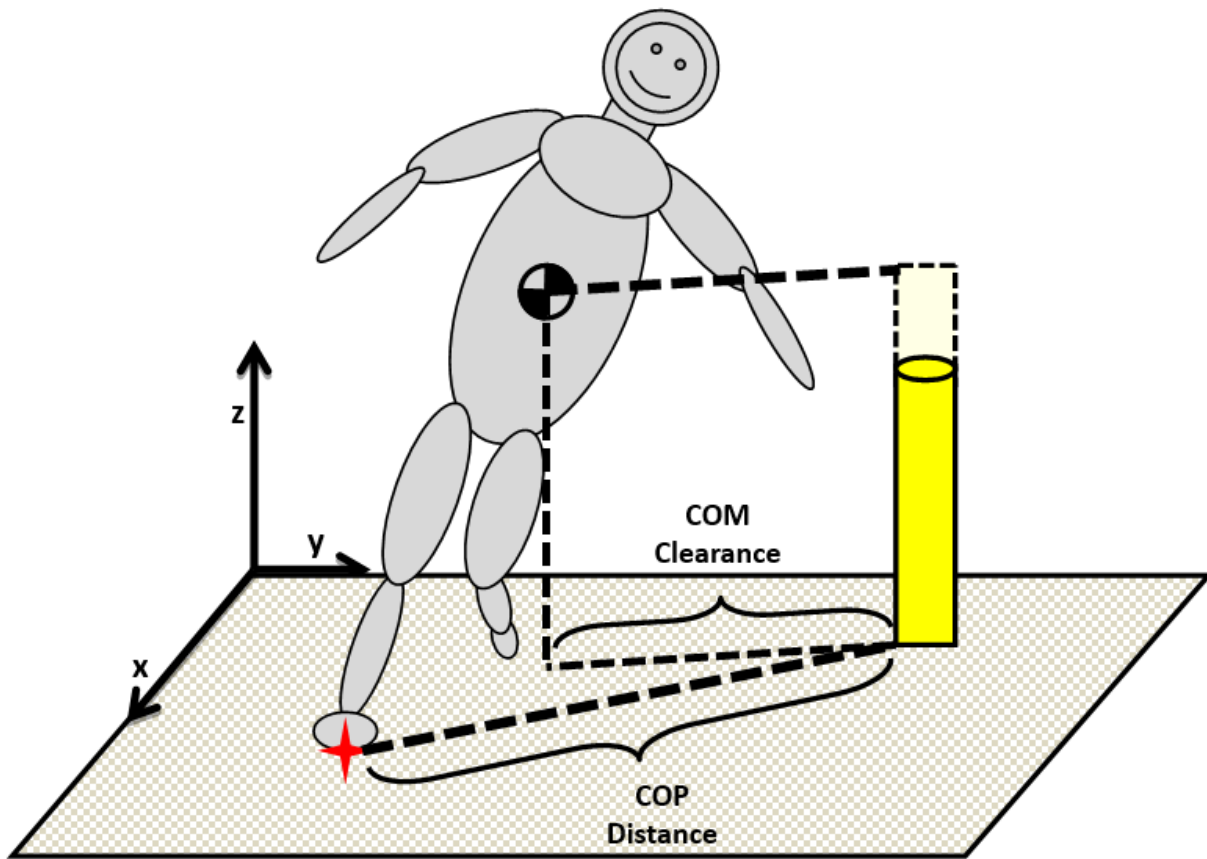


454

455 **Figure 1.** Adopted from Fino and Lockhart (2014). A top-down view of the walkway and  
456 adjoining section with marked start and stop lines, path, and corner pylon. All dimensions given  
457 are in meters. The gray shaded areas indicate the locations of the force plates. The green shaded  
458 area indicates the area covered in Micropore tape.

459

460 Figure 2



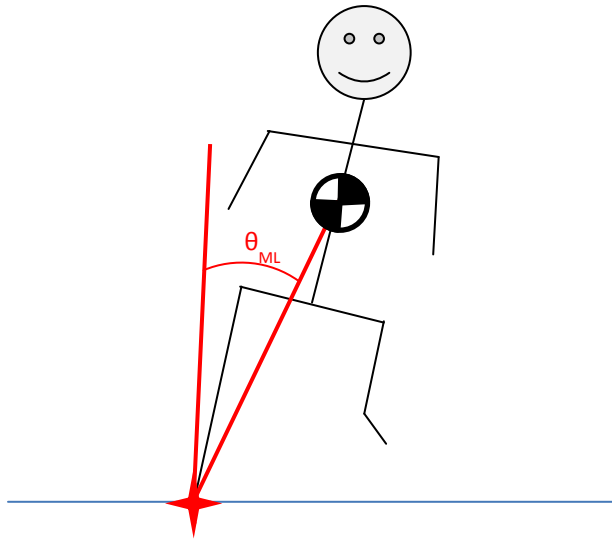
461

462 **Figure 2.** Depiction of COM clearance and COP distance calculations. The COM clearance was  
463 the planar distance from the whole body COM to the pylon (yellow) or pylon projection to the  
464 COM horizontal plane. The COP (red star) distance was the horizontal distance from the COP to  
465 the base of the pylon.

466

467

468 **Figure 3**

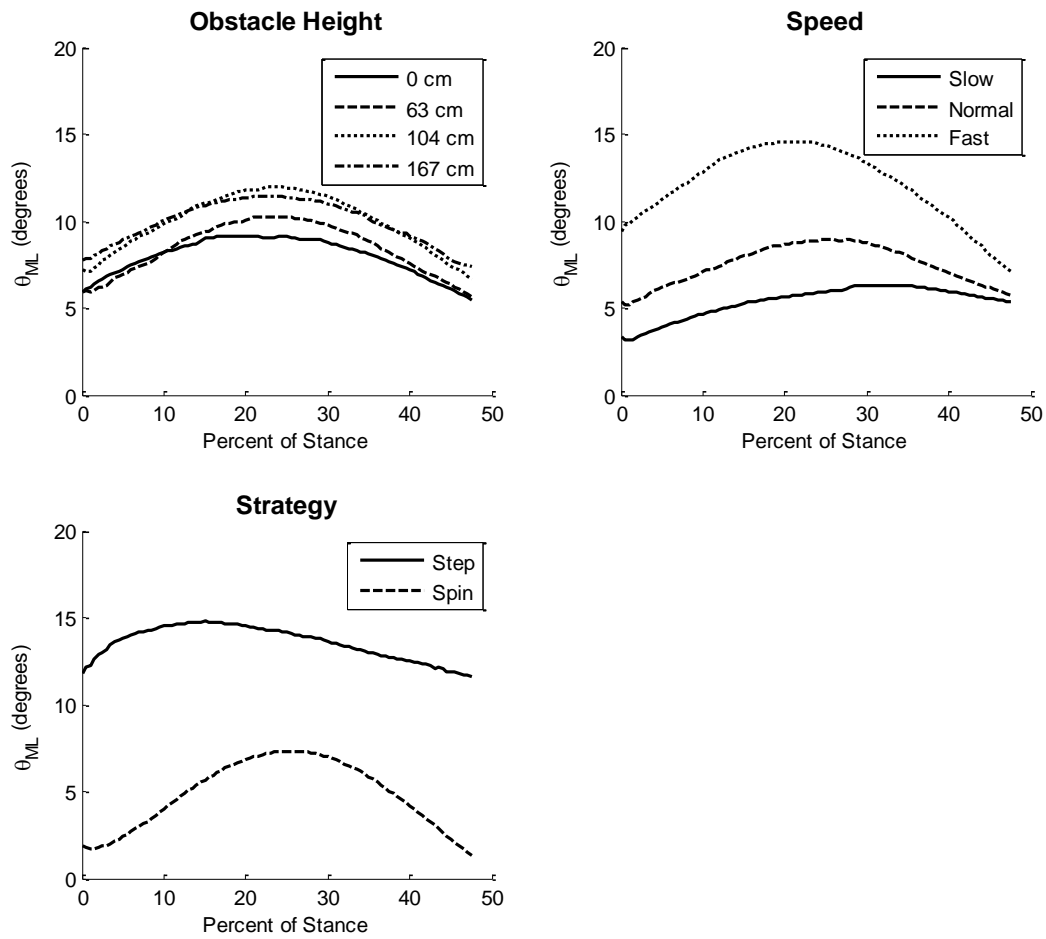


469

470 **Figure 3.** Diagram of the mediolateral COM-COP angle  $\theta_{ML}$ . The ML COM-COP angle was the  
471 angle between the vertical and the line connecting the COM to the COP (red star) as seen from  
472 the frontal plane of the participant. The frontal plane and participant-fixed coordinate frame was  
473 defined by the orientation of the hips using the iliac crest and trochanter markers on each side of  
474 the body.

475

476 Figure 4



477

478 **Figure 4.** Population average plots of  $\theta_{ML}$  for the first half of the turning stance for each obstacle  
479 height (top-left), speed (top-right), and strategy (bottom-left). Values reported in Tables 1 and 3  
480 reflect means at weight acceptance, which occurred at an average of 10% of stance.

481





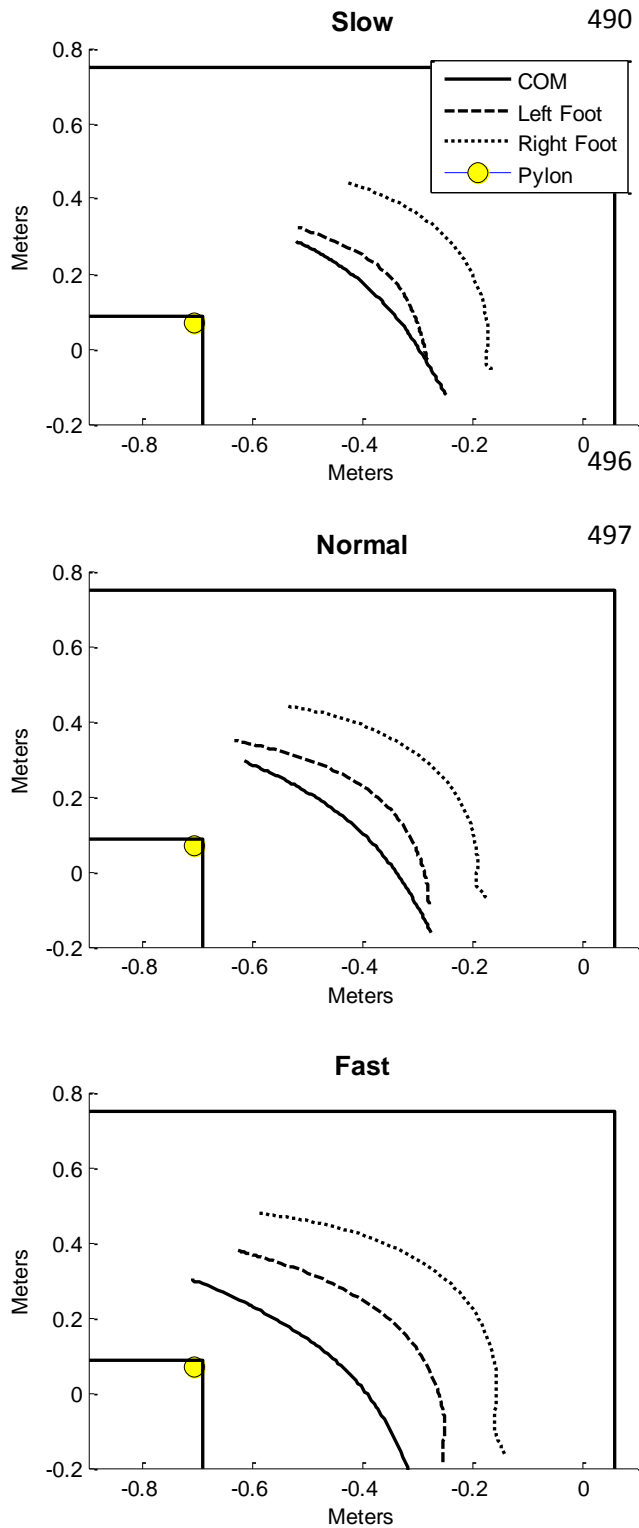
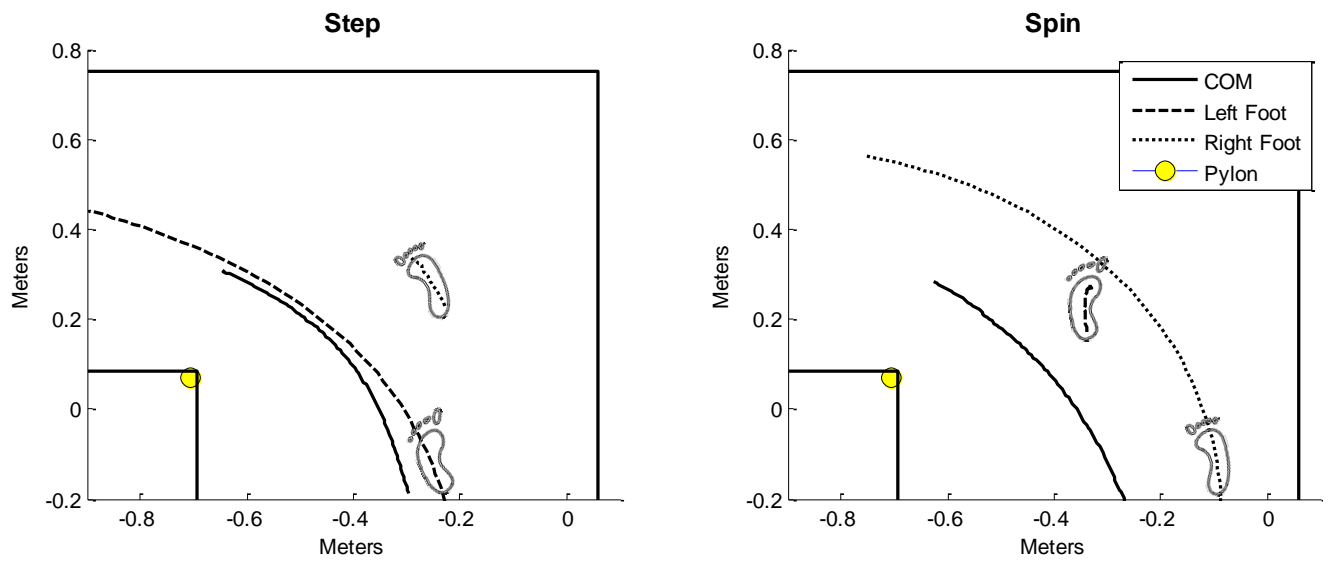


**Figure 6.** Population average plots for the whole body (solid line), left foot (dashed line), and right foot (dotted line) COM trajectories over the first half of stance phase for each speed. The COM displacement outside the BOS increases as speed increases, but even at slow speeds the COM travels outside the BOS.

499 Figure 7



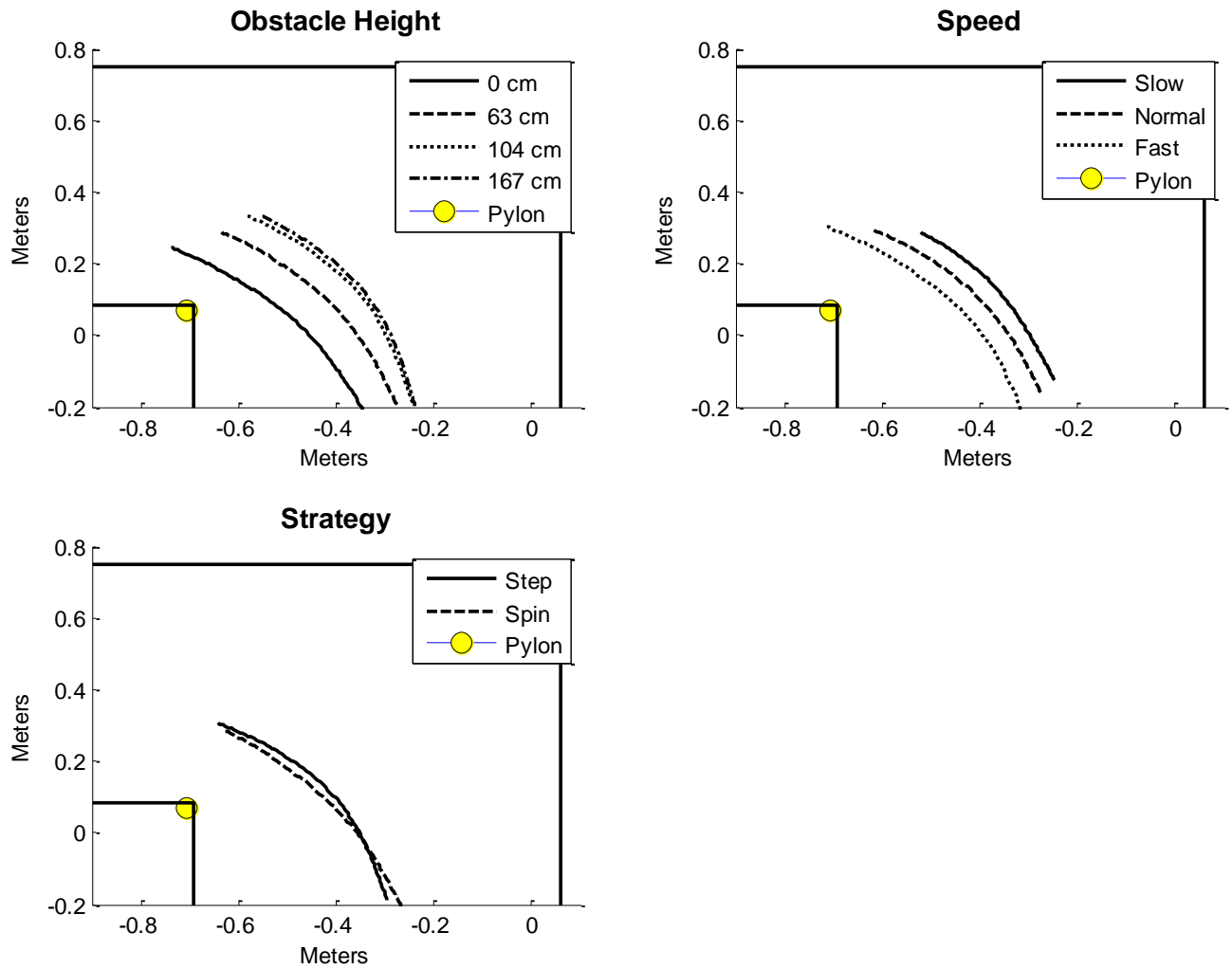
500  
501

502 **Figure 7.** Population average plots for the whole body (solid line), left foot (dashed line), and  
503 right foot (dotted line) COM trajectories over the first half of stance phase for each strategy with  
504 representative foot placement. The stance limb for step turns to the left is the right leg, while for  
505 spin turns to the left it is the left leg which results in small path lengths for those respective  
506 trajectories. For both trajectories, the COM falls outside the BOS for the entire first half of  
507 stance. The COM displacement outside the BOS is much higher during spin turns than step turns.

508

509 Figure 8

510



511

512 **Figure 8.** Population average plots for the COM trajectories separated by variable to show the

513 different trajectories' average curvatures.

514

515

516

517 **Table 1**

518

**Table 1**

Results from the univariate descriptive statistics: Means and standard deviations for minimum COM clearance, COP distance, RCOF at weight acceptance, and  $\theta_{ML}$  by speed, height, and turning strategy. The medians and inter-quartile bounds (Q1, Q3) are presented for curvature.

	Number of Trials*	COM Clearance (m)		COP Radius (m)		RCOF		$\theta_{ML}$ (degrees)		Curvature	
		Mean	St Dev	Mean	St Dev	Mean	St Dev	Mean	St Dev	Median	[Q1, Q3]
<b>Speed (self-selected)</b>											
Slow	92	0.28	0.09	0.45	0.12	0.27	0.07	4.4	6.0	8.7	[4.8, 14.0]
Normal	156	0.25	0.10	0.46	0.14	0.30	0.07	6.8	6.1	6.9	[4.5, 11.1]
Fast	181	0.21	0.10	0.51	0.13	0.41	0.08	12.7	7.0	6.5	[4.0, 10.9]
<b>Height (cm)</b>											
0	129	0.15	0.09	0.36	0.13	0.32	0.09	8.1	7.0	4.7	[2.4, 7.3]
63	111	0.23	0.08	0.47	0.11	0.33	0.09	7.6	6.7	5.5	[3.9, 10.3]
104	105	0.30	0.06	0.55	0.10	0.35	0.09	9.3	7.9	8.4	[5.9, 13.2]
167	84	0.33	0.05	0.57	0.09	0.36	0.10	10.4	7.6	10.6	[7.6, 16.1]
<b>Turning Strategy</b>											
Step	205	0.25	0.10	0.53	0.13	0.35	0.09	14.6	5.0	9.6	[5.7, 14.6]
Spin	224	0.23	0.10	0.43	0.12	0.33	0.09	3.4	4.4	5.3	[3.5, 8.8]

\*Number of trials analyzed after excluding trials with improper foot placement or multiple steps on the force plate

519

520

## 521 Table 2

522

**Table 2**

Average approach speeds for each self-selected speed. Average turning speeds are separated by each variable.

	Number of Trials	Approach Speed (m/s)		Turning Speed (m/s)	
		Mean	Std	Mean	Std
<b>Speed (self-selected)</b>					
Slow	92	0.93	0.28	1.10	0.24
Normal	156	1.43	0.36	1.27	0.26
Fast	181	2.03	0.27	1.65	0.25
<b>Height (cm)</b>					
0	129	1.48	0.57	1.36	0.33
63	111	1.45	0.54	1.36	0.35
104	105	1.49	0.57	1.41	0.35
167	84	1.45	0.56	1.44	0.33
<b>Turning Strategy</b>					
Step	205	1.47	0.54	1.40	0.35
Spin	224	1.46	0.58	1.37	0.33

523

Table 3

**Table 3**

Results from GEE models for outcomes: minimum COM clearance, COP distance, RCOF at weight acceptance, and  $\theta_{ML}$  by speed, height, and turning strategy. The beta coefficients show the mean differences between each category and the reference. The model intercept ( $\beta_0$ ) is also presented as the mean outcome at a normal speed, 0 cm height, and a step turning strategy. The significance level was set at 0.05.

		COM Clearance (m)		COP Radius (m)		RCOF		$\theta_{ML}$ (degrees)		Curvature	
Number of Trials		Beta (SE)	P Value	Beta (SE)	P Value	Beta (SE)	P Value	Beta (SE)	P Value	Beta (SE)	P Value
<b>Intercept</b>		0.25 (0.10)	<0.0001	0.40 (0.01)	<0.0001	0.29 (0.01)	<0.0001	12.19 (0.42)	<0.0001	1.77 (0.09)	<0.0001
<b>Speed (self-selected)</b>											
Slow	92	0.04 (0.01)	<0.0001*	0.002 (0.01)	0.8264	-0.03 (0.01)	0.0040*	-2.13 (0.45)	<0.0001*	0.42 (0.13)	0.0009*
Normal	156		Ref.		Ref.		Ref.		Ref.		Ref.
Fast	182	-0.05 (0.01)	<0.0001*	0.04 (0.01)	<0.0001*	0.11 (0.01)	<0.0001*	5.78 (0.38)	<0.0001*	-0.23 (0.10)	0.0200*
<b>Height (cm)</b>											
0	130		Ref.		Ref.		Ref.		Ref.		Ref.
63	111	0.08 (0.01)	<0.0001†	0.12 (0.01)	<0.0001†	0.02 (0.01)	0.0651	0.15 (0.45)	0.7457	0.35 (0.08)	<0.0001†
104	105	0.16 (0.01)	<0.0001†	0.19 (0.01)	<0.0001†	0.02 (0.01)	0.0123†	0.85 (0.46)	0.0633	0.72 (0.08)	<0.0001†
167	84	0.19 (0.01)	<0.0001†	0.21 (0.01)	<0.0001†	0.03 (0.01)	0.0010†	0.96 (0.49)	0.0488†	0.93 (0.09)	<0.0001†
<b>Turning Strategy</b>											
Step	205		Ref.		Ref.		Ref.		Ref.		Ref.
Spin	225	-0.02 (0.01)	0.0141‡	-0.10 (0.01)	<0.0001‡	-0.02 (0.01)	0.0062‡	-11.05 (0.34)	<0.0001‡	-0.57 (0.10)	<0.0001‡
<b>Speed*Strategy Interactions</b>											
Slow * Spin		-	-	-	-	-	-	-	-	-0.31 (0.17)	0.0634
Fast * Spin		-	-	-	-	-	-	-	-	0.20 (0.13)	0.1378

---

\* Significantly different than normal speed  
† Significantly different than 0 cm height (no obstacle)  
‡ Significantly different than step turn

525